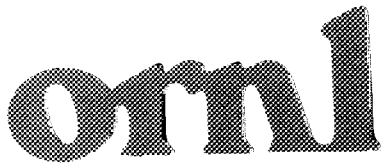


MARTIN MARIETTA ENERGY SYSTEMS LIBRARIES



3 4456 0377032 8

ORNL/TM-12200



OAK RIDGE
NATIONAL
LABORATORY

MARTIN MARIETTA

Alloying Effects on Mechanical and Metallurgical Properties of NiAl

C. T. Liu
J. A. Horton
E. H. Lee
E. P. George

MANAGED BY
MARTIN MARIETTA ENERGY SYSTEMS, INC.
FOR THE UNITED STATES
DEPARTMENT OF ENERGY

OAK RIDGE NATIONAL LABORATORY
CENTRAL RESEARCH LIBRARY
CIRCULATION SECTION
KOBEN ROOM 175

LIBRARY LOAN COPY

DO NOT TRANSFER TO ANOTHER PERSON

If you wish someone else to use this report, send in name with report and the library will arrange a loan.

NOV 20 1963

This report has been reproduced directly from the best available copy.

Available to DOE and DOE contractors from the Office of Scientific and Technical Information, P.O. Box 62, Oak Ridge, TN 37831; prices available from (615) 576-8401, FTS 626-8401.

Available to the public from the National Technical Information Service, U.S. Department of Commerce, 5285 Port Royal Rd., Springfield, VA 22161.

This report was prepared as an account of work sponsored by an agency of the United States Government. Neither the United States Government nor any agency thereof, nor any of their employees, makes any warranty, express or implied, or assumes any legal liability or responsibility for the accuracy, completeness, or usefulness of any information, apparatus, product, or process disclosed, or represents that its use would not infringe privately owned rights. Reference herein to any specific commercial product, process, or service by trade name, trademark, manufacturer, or otherwise, does not necessarily constitute or imply its endorsement, recommendation, or favoring by the United States Government or any agency thereof. The views and opinions of authors expressed herein do not necessarily state or reflect those of the United States Government or any agency thereof.

Metals and Ceramics Division

**ALLOYING EFFECTS ON MECHANICAL AND
METALLURGICAL PROPERTIES OF NiAl**

C. T. Liu
J. A. Horton
E. H. Lee
E. P. George

Date Prepared: October 1990

Date Published: June 1993

NOTICE: This document contains information of a preliminary nature. It is subject to revision or correction and therefore does not represent a final report.

Prepared for the
U.S. Department of Energy
Assistant Secretary for Conservation and Renewable Energy
Office of Industrial Technologies
Advanced Industrial Concepts Materials Program
ED 38 02 00 0

Prepared by the
OAK RIDGE NATIONAL LABORATORY
Oak Ridge, Tennessee 37831-6285
managed by
MARTIN MARIETTA ENERGY SYSTEMS, INC.
for the
U.S. DEPARTMENT OF ENERGY



TABLE OF CONTENTS

	<u>Page</u>
LIST OF FIGURES	v
LIST OF TABLES	vii
ABSTRACT.....	1
1. INTRODUCTION	1
2. MICROALLOYING OF STOICHIOMETRIC NiAl.....	2
3. PREPARATION AND FABRICATION OF MACROALLOYED NiAl	3
4. EFFECTS OF ALLOY ADDITIONS (EXCLUDING Mo, W, AND V).....	6
5. ALLOYING EFFECTS OF Mo, W, AND V	6
6. INITIAL ALLOY DEVELOPMENT OF NiAl ALLOYS.....	15
7. TEM STUDY OF NiAl ALLOYS	17
8. CREEP PROPERTIES OF NiAl ALLOYS	22
9. OXIDATION PROPERTIES	22
10. SUMMARY AND CONCLUSIONS.....	24
11. ACKNOWLEDGMENTS.....	26
12. REFERENCES.....	26

LIST OF FIGURES

<u>Figure</u>		<u>Page</u>
1	The location of alloying elements (added to NiAl) in a modified periodic chart.....	4
2	Optical micrograph of NiAl alloys: (a) NAL-41, NiAl + 5% Fe, annealed 1 h at 900°C, and (b) NAL-48, NiAl + 0.4% Ti, annealed 1 h at 1000°C	8
3	Optical micrographs of NAL-44 (NiAl + 0.4% Mo): (a) anneal 1 h at 1000°C, partially recrystallized, and (b) anneal 1 h at 1200°C, completely recrystallized.....	9
4	Back-scattered electron micrograph showing the formation of molybdenum-rich particles in NAL-55 (NiAl + 0.7% Mo).....	11
5	SEM fractograph of NAL-44 (NiAl + 0.4% Mo) annealed 1 h at 1200°C, showing a mixed fracture mode	12
6	Comparison of tensile properties of stoichiometric NiAl with the alloy NAL-44 containing 0.4% Mo	13
7	SEM fractograph of NAL-61 (NiAl + 1.5% Mo + 0.4% Ta, at. %) fractured at room temperature	16
8	Microstructure of NAL-59 (NiAl + 1.5% Mo + 0.4% Nb, at. %) annealed for 1 h at 1300°C: (a) optical micrograph and (b) back-scattered electron micrograph	18
9	TEM micrograph of alloy NAL-55 after an anneal of 1 h at 1200°C and a strain of 1.3% showing precipitate and dislocation distribution	19
10	TEM micrograph of alloy NAL-61 after an anneal of 1 h at 1300°C and a strain of 2.9%.....	20
11	TEM micrograph of a dislocation spiral in NAL-59 that nucleated on a second-phase precipitate from a vacancy condensation mechanism. The spiral is a prismatic edge loop with a Burgers vector of [001]. Figure 11 (a) is looking straight on the [001] habit plane of the spiral. The dislocation is in residual contrast since $g \cdot b = 0$. In Fig. 11 (b), the specimen is tilted so that the intersection of the spiral with the precipitate can be seen. The electron beam direction is [101] and $g = [\bar{1}01]$	21
12	Plot of weight change as a function of exposure time for NiAl alloys exposed to air at 800°C	25

Figure

Page

13	Plot of weight change as a function of exposure time for NiAl alloys exposed to air at 1000°C.....	25
----	---	----

LIST OF TABLES

<u>Table</u>		<u>Page</u>
1	Alloying elements added to NiAl	5
2	Tensile properties of NiAl alloys	7
3	Results of electron microprobe analyses of matrix and second-phase particles in NiAl alloys	11
4	Effect of heat treatment on room-temperature tensile properties on NAL-44 (NiAl + 0.4% Mo)	12
5	Effect of molybdenum additions on tensile properties of NiAl alloys	13
6	Effect of boron doping on tensile properties of NiAl containing 0.4 at. % Mo	14
7	Effect of 0.4 at. % vanadium, molybdenum, or tungsten on tensile properties of NiAl	15
8	Tensile properties of complex NiAl alloys	16
9	TEM compositional analysis by EDS	19
10	Creep properties of NiAl alloys tested at 68.9 MPa (10 ksi) and 816°C (1500°F) in air	23
11	Creep properties of NiAl alloys tested at 130 MPa (20 ksi) and 816°C (1500°F).....	23

ALLOYING EFFECTS ON MECHANICAL AND METALLURGICAL PROPERTIES OF NiAl*

C. T. Liu, J. A. Horton, E. H. Lee, and E. P. George

ABSTRACT

Alloying effects have been investigated in near-stoichiometric NiAl for the purpose of improving its mechanical and metallurgical properties. Ternary additions of 19 elements at levels up to 10 at. % were added to NiAl; among them, molybdenum is found to be most effective in improving the room-temperature ductility and high-temperature strength. Alloying with $1.0 \pm 0.6\%$ molybdenum almost doubles the room-temperature tensile ductility of NiAl and triples its yield strength at 1000°C . The creep properties of molybdenum-modified NiAl alloys can be dramatically improved by alloying with up to 1% of niobium or tantalum. Because of the low solubilities of molybdenum and niobium in NiAl, the beneficial effects mainly come from precipitation hardening. Fine and coarse precipitates are revealed by both transmission electron microscopy (TEM) and electron microprobe analyses. Molybdenum-containing alloys possess excellent oxidation resistance and can be fabricated into rod stock by hot extrusion at 900 to 1050°C . This study of alloying effects provides a critical input for the alloy design of ductile and strong NiAl aluminide alloys for high-temperature structural applications.

1. INTRODUCTION

NiAl alloys containing more than 40 at. % nickel form a single-phase B2-type ordered crystal structure based on the body-centered cubic (bcc) lattice.¹ In terms of physical properties, B2-NiAl offers more potential for high-temperature applications than $\text{L1}_2\text{-Ni}_3\text{Al}$. It has a higher melting point ($T_m = 1638^{\circ}\text{C}$ for NiAl vs 1395°C for Ni_3Al), a substantially lower density (5.86 g/cc vs 7.50 g/cc), and a higher Young's modulus (42.7×10^6 vs 25.9×10^6 psi). In addition, NiAl offers excellent oxidation resistance at high temperatures.^{2,3} In

*Research sponsored by the U.S. Department of Energy, Assistant Secretary for Conservation and Renewable Energy, Office of Industrial Technologies, Advanced Industrial Concepts (AIC) Materials Program, under contract DE-AC05-84OR21400 with Martin Marietta Energy Systems, Inc.

the 1950s and 1960s, NiAl alloys were used as a coating material for hot components in corrosive environments. The oxidation resistance of NiAl can be further improved by alloying with yttrium and other refractory elements such as hafnium and zirconium.^{4,5}

The use of NiAl as structural members, however, suffers from two major drawbacks: (1) poor ductility at ambient temperatures and (2) low strength and creep resistance at elevated temperatures. Single crystals of NiAl are quite ductile in compression, but both single and polycrystalline NiAl appear to be brittle in tension at room temperature.⁶⁻⁸ The nickel aluminide exhibits mainly $\langle 100 \rangle$ slip,⁹⁻¹¹ rather than the $\langle 111 \rangle$ slip that is commonly observed for bcc materials. The lack of sufficient slip systems has been regarded as a major cause for the low ductility of NiAl.⁶⁻⁸ The aluminide shows a sharp increase in ductility above 400°C and becomes very ductile above 600°C.^{12,13} Hence, there is no major problem in the fabrication of NiAl. At higher temperatures, NiAl is highly ductile but weak in strength. For instance, Ni-50 at. % Al has a yield strength of 35 MPa and a tensile ductility of >50% at 1000°C.

During the past 30 years, considerable effort has been devoted to improving the ductility of NiAl alloys at ambient temperatures.^{6-8,12} After an early report in 1966 of limited (2%) room-temperature tensile ductility in polycrystalline NiAl,¹⁴ numerous later attempts to reproduce this ductility were unsuccessful until Hahn and Vedula¹³ recently showed that it was possible to obtain room-temperature plastic elongation of 2.5% in nearly stoichiometric, cast and extruded NiAl. Although it is not completely clear why the previous attempts were unsuccessful, it is now routinely possible to obtain plastic elongations of 2 to 3% in cast and extruded stoichiometric NiAl.^{15,16} Perhaps some of the earlier unsuccessful attempts, especially those using the powder metallurgy approach,¹⁷ were plagued by interstitial element problems. Small deviations from stoichiometry, however, result in a complete loss of the tensile ductility.¹³ This embrittlement effect has been attributed to point defects generated in off-stoichiometric NiAl.^{15,16} It is known that deviations from stoichiometry are accommodated by the incorporation of vacancies in aluminum-rich alloys and by formation of anti-site defects in nickel-rich NiAl.¹⁸⁻²¹ The presence of these defects substantially hardens NiAl at ambient temperatures,²² thereby reducing its ductility.^{15,16}

2. MICROALLOYING OF STOICHIOMETRIC NiAl

This section briefly summarizes our work on microalloying of NiAl.^{15,16} The fracture mode of polycrystalline NiAl with the stoichiometric composition is predominantly intergranular at ambient temperatures. Our detailed Auger analyses showed that grain

boundaries in NiAl are extremely clean and free of impurities. This implies that grain boundaries in NiAl are intrinsically brittle, like those in Ni₃Al.²³⁻²⁵

In an early study, microalloying elements such as B, C, and Be were added to NiAl for improving its fracture behavior.¹⁵ We have found that microalloying with boron at levels to 300 wppm (0.12 at. %) is able to completely suppress this intergranular fracture. Auger analysis confirmed that the beneficial effect of boron is due to its strong segregation at grain boundaries. Unlike in Ni₃Al,^{23, 26-27} however, the suppression of grain-boundary fracture is not accompanied by an increase in ductility. On the contrary, because of its strong solid-solution strengthening effect in NiAl, addition of too much boron can actually cause embrittlement.^{15,16}

A measurement of the yield strength as a function of boron concentration yields a solid-solution hardening value of ~4500 MPa/at. % B, due to boron additions. Thus, boron is an extremely potent solid-solution strengthener in NiAl. As a result, any potential benefit of improved grain-boundary strength is more than offset by an increase in yield strength. For instance, if greater than about 100 wppm boron (0.04 at. % B) is added to NiAl, the aluminate fractures by transgranular cleavage before macroscopic yielding can take place. The observation of cleavage fracture suggests that poor cohesive strength across crystallographic planes is another major cause for brittle fracture and low ductility of NiAl.^{15,16}

Unlike boron, both carbon (300 wppm) and beryllium (500 wppm) are ineffective in suppressing intergranular fracture in NiAl, and Auger analyses of the carbon-doped alloy revealed that carbon did not affect the fracture mode because it did not segregate to the grain boundaries.¹⁵ Although neither beryllium nor carbon suppresses grain-boundary fracture, their effects on the tensile ductility of NiAl were quite different. The ductility of the beryllium-doped alloy was higher than that of the boron-doped alloy because beryllium, unlike boron, has a rather modest strengthening effect in NiAl, whereas the carbon-doped alloy was brittle like the boron-doped alloy because carbon is a potent solid-solution strengthener, just like boron. These observations were rationalized by considering a hard-sphere model for interstitial and substitutional sites in NiAl.¹⁵ Our studies also showed that the nickel and aluminum concentrations of the grain boundaries were not significantly different from the bulk levels, and no evidence was found for Ni-B cosegregation.^{15,16}

3. PREPARATION AND FABRICATION OF MACROALLOYED NiAl

The foregoing section indicates that microalloying with boron suppresses brittle grain-boundary fracture, but it does not increase the tensile ductility of stoichiometric NiAl.

This suggests the need to improve bulk properties of NiAl, in terms of improved cleavage strength and increased slip systems. Macroalloying was thus adopted in this study to alter the bulk properties at room and elevated temperatures.

In this study, 12 elements were selected for alloying with NiAl. The selection of alloying elements was based on considerations of electronic structure, atom bonding, solubility limit, and antiphase boundary (APB) energy. The location of these elements is shown in a modified periodic chart,²⁸⁻³⁰ which ranges from groups IIIA to IIIB (see Fig. 1).

NiAl alloys containing up to 10 at. % of the alloying elements were prepared by arc melting using commercial-purity nickel, aluminum, and alloying metals. The elements listed in Table 1 were chosen to replace nickel, aluminum, or both, based on their chemical behavior.

ORNL-DWG 90-14946

0	1A											IIB	IIIB	IVB	VB	VIB	VIIB
1	12											77	86	95	100	101	102
He	Li											Be	B	C	N	O	F
2	11	IIA IIIA IVA VA VIA VIIA VIIIa VIIIb VIIIc IB										73	80	85	90	94	99
Ne	Na											Mg	Al	Si	P	S	Cl
3	10	16	19	51	54	57	60	61	64	67	72	76	81	84	89	93	98
Ar	K	Ca	Sc	Ti	V	Cr	Mn	Fe	Co	Ni	Cu	Zn	Ga	Ge	As	Se	Br
4	9	15	25	49	53	56	59	62	65	69	71	75	79	83	88	92	97
Kr	Rb	Sr	Y	Zr	Nb	Mo	Tc	Ru	Rh	Pd	Ag	Cd	In	Sn	Sb	Te	I
5	8	14		50	52	55	58	63	66	68	70	74	78	82	87	91	96
Xe	Cs	Ba		Hf	Ta	W	Re	Os	Ir	Pt	Au	Hg	Tl	Pb	Bi	Po	At
6	7	13															
Rn	Fr	Ra															

Fig. 1. The location of alloying elements (added to NiAl) in a modified periodic chart.

Table 1. Initial alloying elements added to NiAl

Elements	Concentration (at. %)						
Fe	2.0 ^a	2.0 ^c	5.9 ^a	10.0 ^a			
Mo	0.2 ^a	0.4 ^a	0.7 ^c	1.0 ^c	1.5 ^c	2.0 ^c	3.0 ^c
Cr	1.0 ^a						
Ga	1.0 ^b						
Ti	0.4 ^b						
V	0.4 ^c						
Y	0.0025 ^c						
W	0.4 ^a						
Mn	1.0 ^a						
Cu	2.0 ^a						
Ag	2.0 ^a						
Zn	10.0 ^a	10.0 ^b					

^aSubstitution for Ni atoms.

^bSubstitution for Al atoms.

^cSubstitution for both Ni and Al atoms.

The ingots were drop-cast into cylindrical copper chill molds 25.4 mm in diameter and 102 mm in length. After sectioning the head, the cast ingots were canned in mild steels and extruded at 900°C at a ratio of 9:1. Most alloys were successfully extruded to 8-mm-diam rod stock without difficulty.

Buttonhead tensile specimens with a diameter of 3.2 mm in the 17.8-mm-long gage section were ground from the extruded rods; electropolished for 120 s at 6 to 7 V in a solution of 13% H₂SO₄ in methanol alcohol; and annealed in vacuum for 1 h at various temperatures to produce stress-relieved, partially recrystallized or fully recrystallized grain structures for mechanical property evaluation. Most specimens were given a final anneal of 1 h at 800°C to reduce point defects.

Tensile tests were performed in air at temperatures to 1000°C using a screw-driven Instron machine operated at an engineering strain rate of 2.4×10^{-3} /s. The test temperature was monitored by a Pt/Pt-10% Rh thermocouple. The strain was measured from a strip chart. Subsequently, the fracture surfaces were examined in a JEOL JSM-35CF scanning electron microscope operated at 25 kV. Creep tests were performed on the same type of specimens, and creep stress was calculated based on a dead-load arrangement.

4. EFFECTS OF ALLOY ADDITIONS (EXCLUDING Mo, W, AND V)

All alloys were successfully prepared, except the alloys containing silver and zinc*. Because of extremely high vapor pressures of zinc and silver, evaporation loss during arc melting masked furnace viewports and sometimes even caused a small explosion inside the furnace. All % symbols in this section and remaining sections refer to at. % for clarity. No tensile specimens could be prepared from the hot-extruded rods of the alloys containing 1% Cr, 1% Mn, 2% Cu, or 10% Fe (all at. %) because they cracked during grinding. Consequently, there are no property data available from these alloys. Miracle et al.³¹ reported that chromium and manganese change the slip systems but do not impart any ductility to NiAl.

Alloy specimens, with their nominal composition listed in Table 2, were annealed for 1 h at 880 to 1000°C to produce a recrystallized grain structure for evaluation of their mechanical properties. Figures 2(a) and (b) show the microstructure of the alloys containing 5% Fe and 0.4% Ti. Second-phase particles appear to be present in the 0.4% Ti alloy. Tensile properties of the NiAl alloys tested at room temperature, 600, and 1000°C are summarized in Table 2. Alloying with 2% Fe increases the strength but lowers the ductility at room temperature. Alloying with 5% Fe completely embrittles NiAl. The addition of 2% Fe only slightly strengthens NiAl at 600 and 1000°C.

The NiAl alloy showed a slight increase in room-temperature ductility when alloyed with 1.0% Ga or 0.4% Ti but exhibited a slight decrease in ductility when alloyed with 0.0025% Y. Among the alloying elements listed in Table 2, titanium is most effective in strengthening of NiAl at 600 and 1000°C. All the alloys showed good ductility at elevated temperatures, except for the 2% Fe alloy that fractured with an elongation of only 6.7% at 600°C.

5. ALLOYING EFFECTS OF Mo, W, AND V

Molybdenum at levels up to 3 at. % was added to NiAl to study its alloying effect. Unalloyed NiAl recrystallizes at 800°C after 1 h, while molybdenum additions increase the recrystallization temperature to as high as 1200°C. This is indicated in Fig. 3 where the 0.4% Mo alloy shows a partial recrystallization (~10%) after being annealed at 1000°C and a complete recrystallization at 1200°C. Second-phase particles are observed in Mo-containing

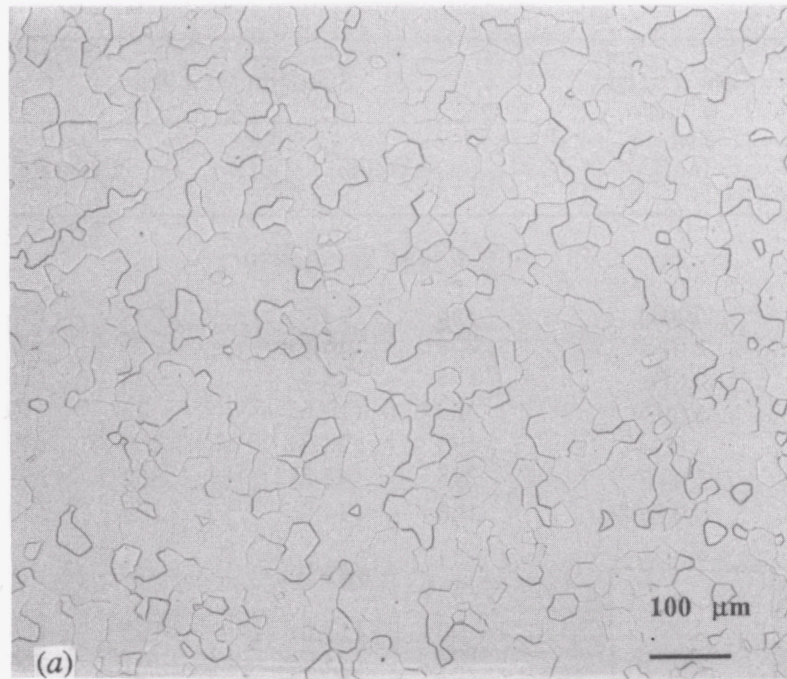
*Zinc was selected as an alloying element based on ab-initio calculations by D. M. Nicholson, Oak Ridge National Laboratory (ORNL).

Table 2. Tensile properties of NiAl alloys

Alloy number	Concentration of alloy element (at.%)	Strength, MPa (ksi)				Elongation (%)
		Yield		Ultimate		
<i>Room temperature</i>						
NAL-31	Base	154	(22.4)	229	(33.3)	2.2
NAL-40	2.0Fe ^a	254	(36.9)	256	(37.1)	0.3
NAL-64	2.0Fe ^c	196	(28.5)	254	(36.8)	1.3
NAL-41	5.0Fe ^a	73	(10.6)	73	(10.6)	0
NAL-47	1.0Ga ^b	195	(28.3)	269	(39.0)	2.6
NAL-48	0.4Ti ^b	295	(42.8)	352	(51.1)	2.6
NAL-50	0.0025Y ^c	165	(24.0)	209	(30.3)	1.5
<i>600 °C</i>						
NAL-31	Base	90	(13.0)	165	(24.0)	58.5
NAL-40	2.0Fe ^a	94	(13.7)	167	(24.2)	6.7
NAL-47	1.0Ga ^b	118	(17.1)	167	(24.3)	86.0
NAL-48	0.4Ti ^b	178	(25.8)	280	(40.6)	35.9
NAL-50	0.0025Y ^c	63	(9.1)	111	(16.1)	50.6
<i>1000 °C</i>						
NAL-31	Base	39	(5.6)	49	(7.1)	59.4
NAL-40	2.0Fe ^a	54	(7.9)	65	(9.5)	78.8
NAL-47	1.0Ga ^b	50	(7.3)	53	(7.7)	74.2
NAL-48	0.4Ti ^b	60	(8.7)	70	(10.1)	78.5
NAL-50	0.0025Y ^c	35	(5.0)	44	(6.4)	72.6

^aSubstitution for Ni atoms.^bSubstitution for Al atoms.^cSubstitution for both Ni and Al atoms.

89-1197



89-0597

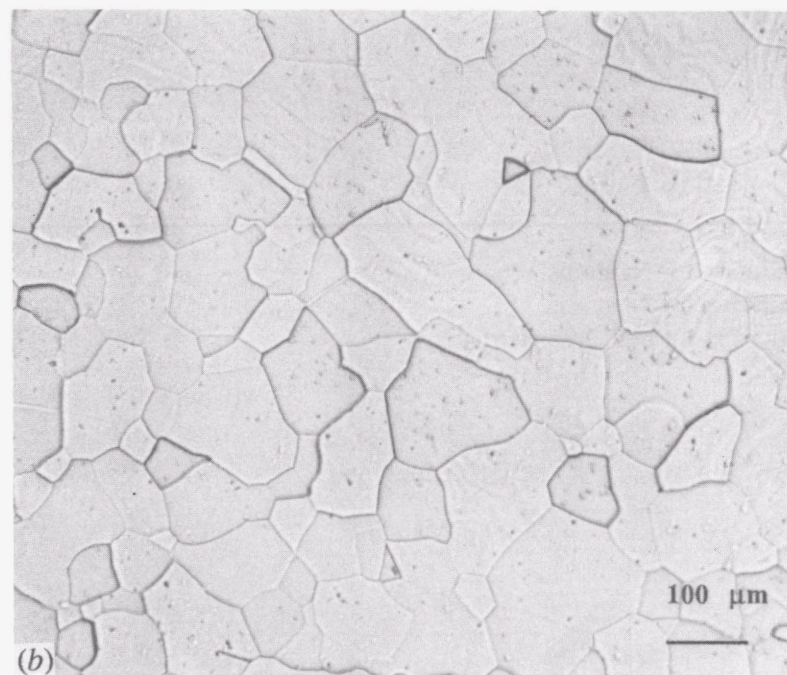
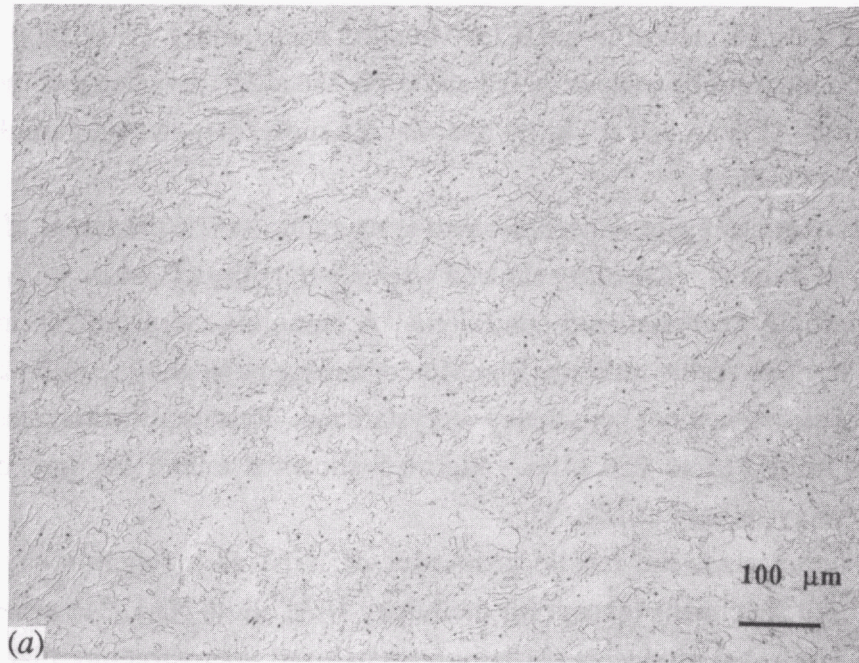


Fig. 2. Optical micrograph of NiAl alloys: (a) NAL-41, NiAl + 5% Fe, annealed 1 h at 900°C, and (b) NAL-48, NiAl + 0.4% Ti, annealed 1 h at 1000°C.

89-0067



89-0238



Fig. 3. Optical micrographs of NAL-44 (NiAl + 0.4% Mo): (a) anneal 1 h at 1000°C, partially recrystallized, and (b) anneal 1 h at 1200°C, completely recrystallized.

alloys, indicating a low solubility of molybdenum in NiAl. Figure 4 shows that both coarse and fine precipitates are present in the 0.7% Mo alloy annealed for 1 h at 1200°C plus 1 h at 800°C. Electron microprobe analysis of 0.2 and 0.7% Mo alloys revealed that the solubility of molybdenum in NiAl is around 0.1 at. % and that the molybdenum-rich particles contain as high as 45% Mo (Table 3).

The effect of annealing treatment on room-temperature tensile properties of the 0.4% Mo alloy is shown in Table 4. The alloy showed a tensile ductility of 3.4 to 3.6% in the stress-relieved and partially recrystallized conditions. A complete recrystallization reduced the ductility to 1.3%. This result indicates that Mo-containing NiAl alloys exhibit a better room-temperature ductility when not completely recrystallized. Recrystallization also lowered the yield strength from 315 to 223 MPa. Figure 5 shows a mixed fracture mode for the 0.4% Mo alloy recrystallized at 1200°C.

Table 5 summarizes the tensile properties of NiAl as a function of molybdenum concentration. All specimens (except for the binary NiAl alloy, NAL-31) were annealed for 1 h at 1000 to 1100°C to produce a partially recrystallized microstructure that gave the best tensile properties. The alloys containing 0.2 to 2.0% Mo showed a room-temperature tensile ductility of 3.3 to 4.4%, which is significantly higher than that of the unalloyed NiAl (2.2%). All Mo-containing alloys are ductile at 600 and 1000°C. Alloying with 0.2% Mo substantially increases the strength of NiAl at all the test temperatures. A further increase in molybdenum to 3 at. % gives only a moderate increase in strength at elevated temperatures. Since the solubility of molybdenum is quite low (~0.1%), the beneficial effect is believed to come from second-phase particles that slow down the recrystallization process and stabilize a wrought structure. Note that the 0.7% Mo alloy (NAL-55) has a yield strength of 121 MPa at 1000°C, which is higher than that of unalloyed NiAl by a factor of three.

Figure 6 is a plot of the tensile properties as a function of temperature for the 0.4% Mo alloy (NAL-44), compared with those of the binary NiAl. The yield strength of both alloys decreases with temperature; however, NAL-44 is stronger than NiAl by more than 100% at all test temperatures. Most importantly, NAL-44 has a tensile ductility better than NiAl at ambient temperatures. The ductility of both alloys increases with temperature above 200°C, and it increases sharply above 400°C. The unalloyed NiAl has a higher ductility above 400°C.

Since microalloying with boron suppresses intergranular fracture,^{15,16} boron at a level of 30 wppm was added to the 0.4% Mo alloy. Table 6 compares the tensile properties of 0.4% Mo alloys with and without boron. The addition of boron appears to slightly increase the ductility and strength at room temperature and 200°C, but it does not affect the tensile properties at higher temperatures.

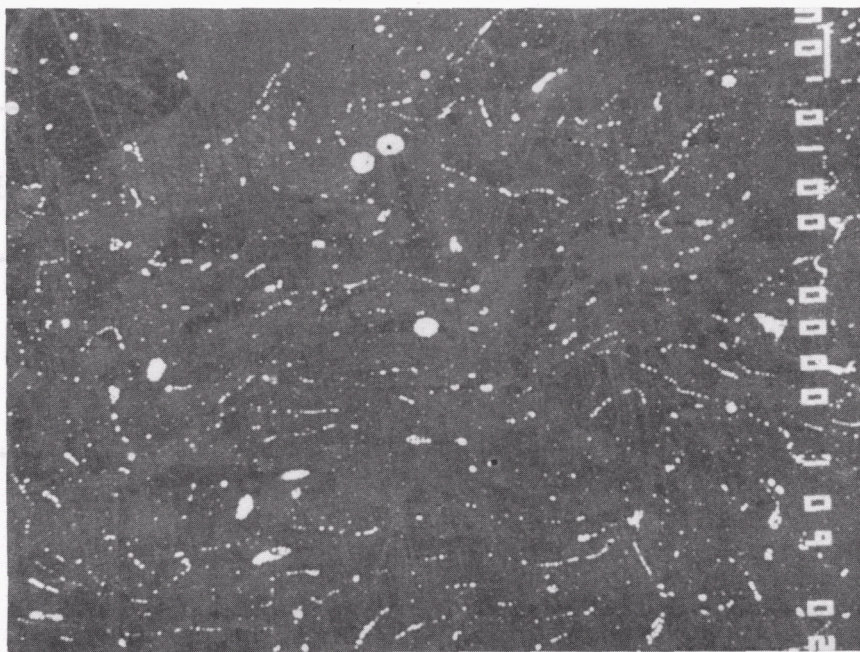


Fig. 4. Back-scattered electron micrograph showing the formation of molybdenum-rich particles in NAL-55 (NiAl + 0.7% Mo).

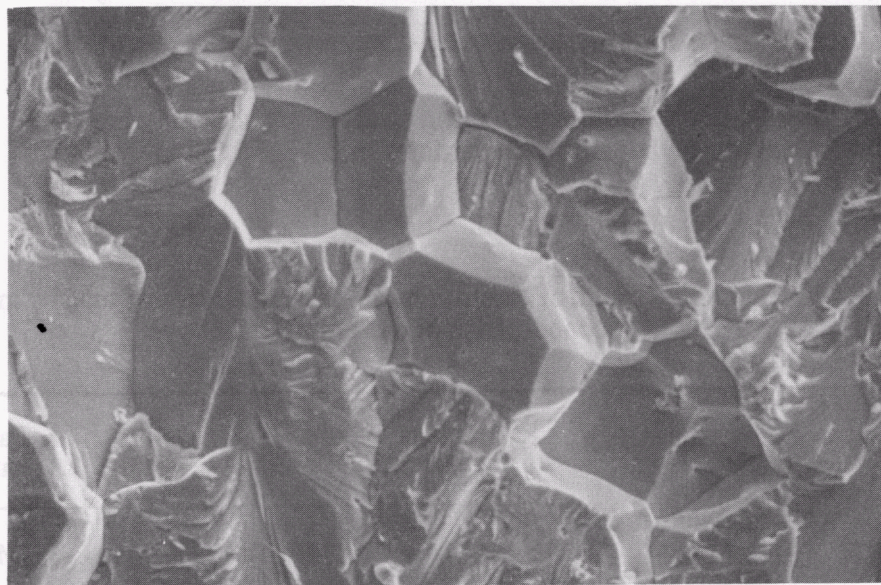
Table 3. Results of electron microprobe analyses of matrix and second-phase particles in NiAl alloys

Alloy number	Alloy concentration (at. %)	Matrix (at. %)			Particle (at. %)		
		Al	Mo/V	Nb/Ta	Al	Mo/V	Nb/Ta
NAL-53	0.2 Mo	50.1	0.06		(I) 25	45	
NAL-55	0.7 Mo	48.1	0.12		(I) 25	45	
NAL-49	0.4 V	48.9	0.38				
NAL-59	1.5 Mo + 0.4 Nb	49.4	0.09	0.00	(I) 10	75	8
					(II) 7	66	18
NAL-62	1.5 Mo + 1.0 Ta	49.9	0.09	0.26	(I) 12	50	20
					(II) 32	6	33

Table 4. Effect of heat treatment on room-temperature tensile properties of NAL-44 (NiAl + 0.4% Mo)

Heat treatment	Strength				Elongation (%)
	Yield		Ultimate		
	MPa	ksi	MPa	ksi	
1 h at 950°C	315	45.7	438	63.6	3.4
1 h at 1000°C	254	36.8	395	57.3	3.6
1 h at 1100°C	227	33.0	355	51.5	3.4
1 h at 1200°C	223	32.3	230	33.4	1.3

M21019



10 μm

Fig. 5. SEM fractograph of NAL-44 (NiAl + 0.4% Mo) annealed 1 h at 1200°C, showing a mixed fracture mode.

Table 5. Effect of molybdenum additions on tensile properties of NiAl alloys

Alloy number	Molybdenum concentration (at.%)	Strength, MPa (ksi)		Elongation (%)
		Yield	Ultimate	
<i>Room temperature</i>				
NAL-31	0	154 (22.4)	229 (33.3)	2.2
NAL-53	0.2	265 (38.5)	425 (61.7)	3.3
NAL-44	0.4	254 (36.8)	395 (57.3)	3.6
NAL-55	0.7	254 (36.8)	425 (61.7)	3.5
NAL-57	1.0	277 (40.2)	460 (66.8)	3.4
NAL-58	1.5	276 (40.1)	486 (70.5)	4.4
NAL-66	2.0	396 (57.5)	551 (80.0)	3.4
NAL-67	3.0	422 (61.2)	530 (76.9)	2.5
<i>600°C</i>				
NAL-31	0	90 (13.0)	165 (24.0)	58.5
NAL-53	0.2	194 (28.2)	277 (40.2)	45.3
NAL-44	0.4	179 (26.0)	259 (37.6)	32.6
NAL-55	0.7	206 (29.9)	297 (43.1)	34.4
NAL-57	1.0	240 (34.9)	324 (47.1)	38.9
NAL-58	1.5	229 (33.3)	304 (44.1)	34.5
<i>1000°C</i>				
NAL-31	0	39 (5.6)	49 (24.0)	58.5
NAL-53	0.2	111 (16.1)	123 (40.2)	45.3
NAL-44	0.4	103 (15.0)	110 (37.6)	32.6
NAL-55	0.7	121 (17.6)	129 (43.1)	34.4
NAL-57	1.0	121 (17.5)	133 (47.1)	38.9
NAL-58	1.5	116 (16.8)	129 (44.1)	34.5
NAL-66	2.0	141 (20.5)	152 (22.1)	40.6
NAL-67	3.0	121 (17.6)	137 (19.9)	42.9

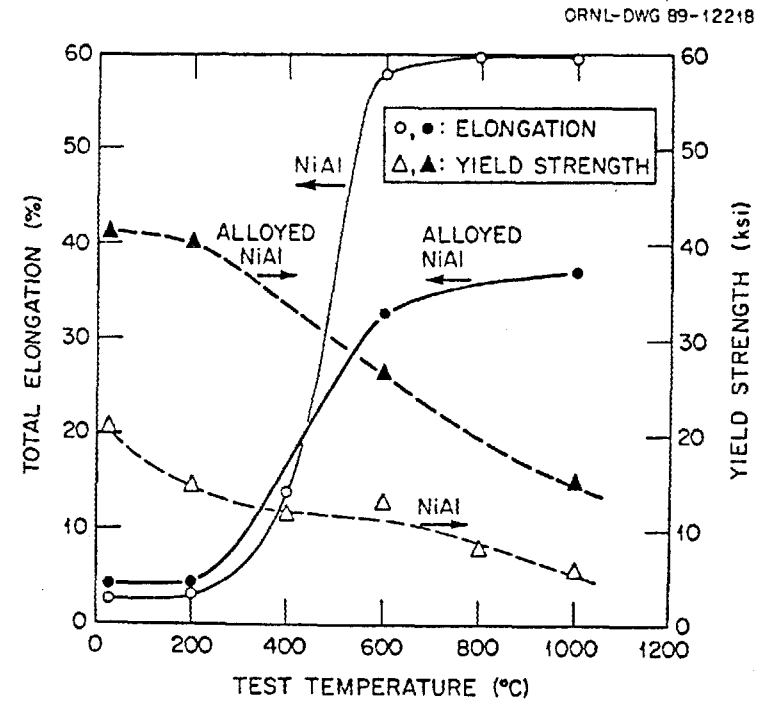


Fig. 6. Comparison of tensile properties of stoichiometric NiAl with the alloy NAL-44 containing 0.4% Mo.

Table 6. Effect of boron doping on tensile properties of NiAl containing 0.4 at. % Mo

Alloy number	Boron concentration (wppm)	Strength, MPa (ksi)				Elongation (%)
		Yield		Ultimate		
<i>Room temperature</i>						
NAL-44	0	254	(36.8)	395	(57.3)	3.6
NAL-55	30	283	(41.1)	461	(66.9)	4.2
<i>200°C</i>						
NAL-44	0	249	(36.2)	371	(53.9)	3.6
NAL-45	30	274	(39.8)	408	(59.2)	4.3
<i>600°C</i>						
NAL-44	0	179	(26.0)	256	(37.6)	32.6
NAL-46	30	182	(26.4)	263	(38.2)	32.6
<i>1000°C</i>						
NAL-44	0	103	(15.0)	110	(15.9)	31.5
NAL-45	30	102	(14.8)	112	(16.3)	36.9

Table 7 compares the tensile properties of NiAl alloys containing 0.4% Mo, W, or V tested at room temperature and 1000°C. Tungsten is most effective in strengthening NiAl, but it appears not to affect the ductility at room temperature. Vanadium is less effective in strengthening NiAl at 1000°C and significantly lowers the room-temperature ductility. Alloying with vanadium, however, improves the creep properties of NiAl, as will be described in Sect. 8.

Unlike the molybdenum- and tungsten-containing alloys, the vanadium-containing alloy is essentially single phase in structure. The electron microprobe analyses in Table 3 showed that NiAl can dissolve more than 0.4% V. Hence, the strengthening effect of vanadium in NiAl-49 must come from solid-solution hardening. Darolia et al.³² recently reported that the addition of vanadium changes the slip behavior but does not impart ductility to NiAl.

Table 7. Effect of 0.4 at. % vanadium, molybdenum, or tungsten on tensile properties of NiAl

Alloy number	Alloying element	Strength, MPa (ksi)				Elongation (%)
		Yield		Ultimate		
<i>Room temperature</i>						
NAL-31	O	154	(22.4)	229	(33.3)	2.2
NAL-44	Mo	254	(36.8)	395	(57.3)	3.6
NAL-51	W	323	(46.9)	449	(65.1)	2.5
NAL-49	V	238	(34.5)	274	(39.8)	1.1
<i>1000 °C</i>						
NAL-31	O	37	(5.6)	49	(7.1)	59.4
NAL-44	Mo	103	(15.0)	110	(15.9)	31.5
NAL-51	W	118	(17.1)	129	(18.7)	32.1
NAL-49	V	64	(9.3)	72	(10.5)	69.0

6. INITIAL ALLOY DEVELOPMENT OF NiAl ALLOYS

The foregoing section indicates that molybdenum is quite effective in improving both the room-temperature ductility and high-temperature strength. As a result, the NiAl alloy containing 1.5 at. % Mo (NAL-58) was chosen as a base for further alloying. The alloying elements Nb, Ta, and V were selected for addition to NAL-58, since they are effective in improving creep resistance.³³ Table 8 lists the alloy compositions based on NAL-58. The alloys were prepared and fabricated in the same way as the earlier alloys, except that an extrusion temperature of 1050, instead of 900°C, was necessary to fabricate a few of the stronger alloys such as NAL-60. The yield strength of NAL-58 is substantially increased by additions of Nb, Ta, and V; however, the increase in strength results in a decrease in the tensile ductility at room temperature. The alloys essentially showed a mixed fracture mode, with transgranular cleavage as the major fracture mode at room temperature (Fig. 7). At 1000°C, niobium is most effective in strengthening and causes no reduction in ductility. The alloy NAL-60 containing 1% Nb has a yield strength five times higher than that of unalloyed NiAl (NAL-31) at 1000°C.

Table 8. Tensile properties of complex NiAl alloys

Alloy number	Alloy concentration (at. %)	Strength, MPa (ksi)		Elongation (%)		
		Yield	Ultimate			
<i>Room temperature</i>						
NAL-31	0	154	(22.4)	229	(33.3)	2.2
NAL-58	1.5 Mo	276	(40.1)	486	(70.5)	4.4
NAL-59	1.5 Mo + 0.4 Nb	325	(47.2)	466	(67.7)	2.8
NAL-60	1.5 Mo + 1.0 Nb	402	(58.3)	431	(62.6)	1.0
NAL-61	1.5 Mo + 0.4 Ta	328	(47.6)	472	(68.5)	2.9
NAL-62	1.5 Mo + 1.0 Ta	388	(56.3)	413	(59.9)	1.3
NAL-72	1.5 Mo + 0.4 V	340	(49.3)	513	(74.4)	3.4
NAL-73	1.5 Mo + 1.0 V	338	(49.1)	494	(71.7)	2.8
<i>1000 °C</i>						
NAL-31	0	39	(5.6)	49	(7.1)	59.4
NAL-58	1.5 Mo	116	(16.8)	129	(18.7)	43.8
NAL-59	1.5 Mo + 0.4 Nb	166	(24.1)	181	(26.2)	35.6
NAL-60	1.5 Mo + 1.0 Nb	195	(28.3)	225	(32.6)	40.5
NAL-61	1.5 Mo + 0.4 Ta	134	(19.4)	146	(21.2)	36.8
NAL-62	1.5 Mo + 1.0 Ta	163	(23.6)	188	(27.3)	27.4
NAL-72	1.5 Mo + 0.4 V					
NAL-73	1.5 Mo + 1.0 V	143	(20.8)	155	(22.5)	41.6

M21020

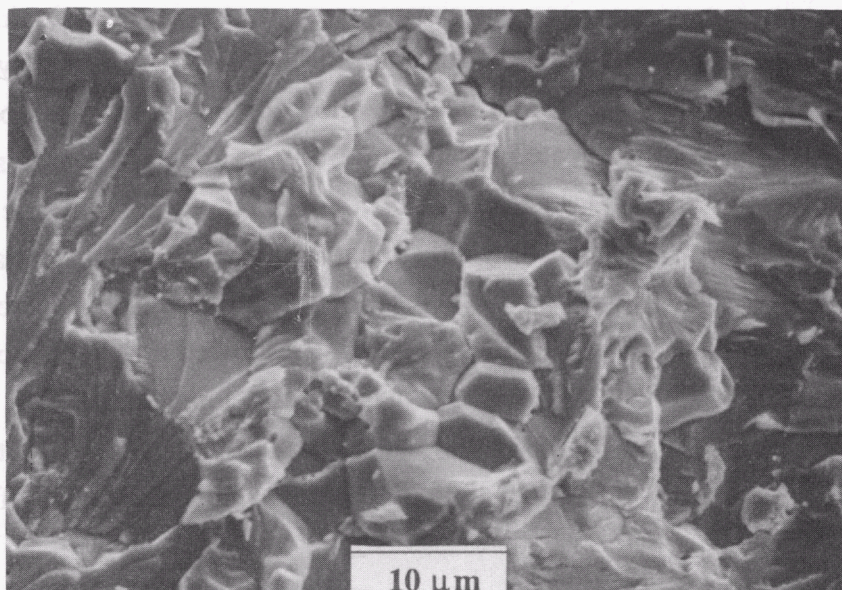


Fig. 7. SEM fractograph of NAL-61 (NiAl + 1.5% Mo + 0.4% Ta, at. %) fractured at room temperature.

Figure 8 shows the grain structure and second-phase particles in NAL-59 after annealing for 1 h at 1300°C. Both coarse and fine particles are observed, and the fine particles are distributed uniformly, while the coarse particles tend to line up and form stringers. The compositions of the matrix and particle phases in NAL-59 containing molybdenum and niobium, and in NAL-62 containing molybdenum and tantalum, were determined by electron microprobe analyses. The results are shown in Table 3. NiAl dissolves about 0.1% Mo and 0.26% Ta, and practically no niobium. Two types of particles are observed in the alloys. Particle (I) contains a higher level of molybdenum (50 to 75%), and particle (II) contains a higher level of Nb/Ta (18 to 33%). Note that alloying with niobium or tantalum does not affect the solubility of Mo, which is about 0.1% in NiAl.

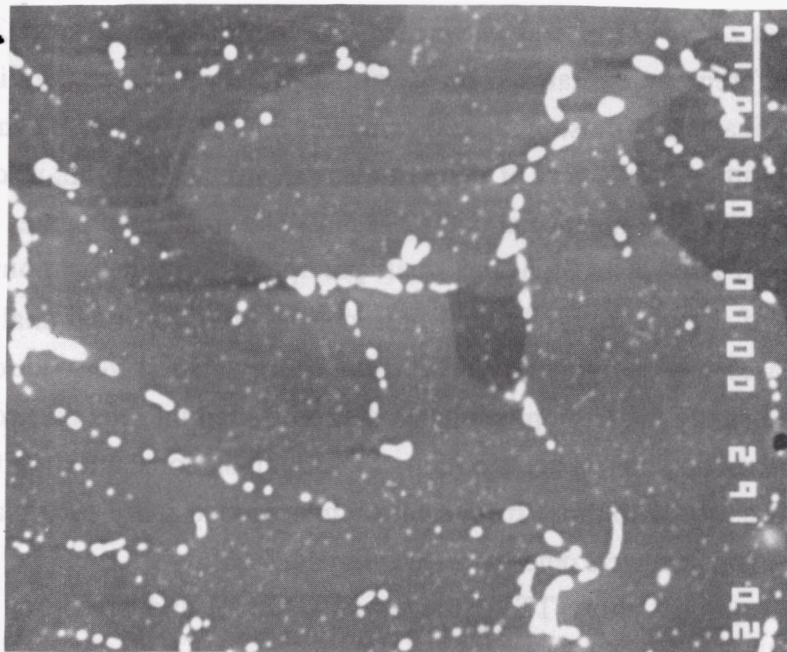
7. TEM STUDY OF NiAl ALLOYS

Three NiAl alloys containing molybdenum, niobium, and tantalum were examined by transmission electron microscopy (TEM). The alloys are NAL-55 containing 0.7% Mo, NAL-59 containing 1.5% Mo and 0.4% Nb, and NAL-61 containing 1.5% Mo and 0.4% Ta. Alloy specimens were annealed for 1 h at 1200 to 1300°C and then deformed in tension at room temperature. TEM disks were sectioned from the tensile specimens and then electropolished in a solution of 10% perchloric acid and 90% methanol at a temperature of -30°C and at 22 V. TEM was performed on Philips CM12 and CM30 microscopes. A number of different precipitates formed with a range in sizes. Preliminary diffraction information indicates that most of these precipitates retain the bcc or B2 structure with a small unit cell. The lattice parameters of the particles are around 0.31 nm, as compared to the B2 matrix with a lattice parameter of about 0.283 nm. The small precipitates ranged in size from 0.25 to 1 μm . It is expected that the small precipitates pin dislocations and contribute to strengthening of these alloys. Table 9 presents the compositional analyses of matrix and precipitate phases, as determined by TEM using energy dispersive spectroscopy (EDS). The analyses were usually made on precipitates that protruded into the electropolishing hole and thereby minimized any matrix contributions. The compositional analyses from TEM/EDS are reasonably consistent with those from electron microprobe analyses in Table 3. Some small particles containing lead were detected in the alloy NAL-61.

Figures 9 and 10 show TEM images of NAL-55 and NAL-61, respectively. The specimen in Fig. 9 was strained 1.3% at room temperature, while the specimen in Fig. 2 was strained 2.9%. Many dislocation loops are present throughout the microstructure of all the



(a)

100 μm 

(b)

10 μm

Fig. 8. Microstructure of NAL-59 (NiAl + 1.5% Mo + 0.4% Nb, at. %) annealed for 1 h at 1300°C: (a) optical micrograph and (b) back-scattered electron micrograph.

Table 9. TEM compositional analysis by EDS

Alloy number	Composition of phases (at. %)			
NAL-55 ^a	<u>Aluminum</u>	<u>Nickel</u>	<u>Molybdenum</u>	
PPT (I)	26	27	47	
PPT (II)	10	5	85	
Matrix	49	51	--	
Nominal	49.65	49.65	0.7	
NAL-59 ^b	<u>Aluminum</u>	<u>Nickel</u>	<u>Molybdenum</u>	<u>Niobium</u>
PPT (I)	24	11	57	8
PPT (II)	30	15	32	23
PPT (III)	38	34	24	4
Matrix	49.5	50.5	--	--
Nominal	49.05	49.05	1.5	0.4
NAL-61 ^c	<u>Aluminum</u>	<u>Nickel</u>	<u>Molybdenum</u>	<u>Tantalum</u>
PPT (I)	8	7	70	15
Matrix	49	51	--	--
Nominal	49.05	49.05	1.5	0.4

^aNi-50Al-0.4Mo (at. %) annealed for 1 h at 1200°C.

^bNi-49.05Al-1.5Mo-0.4Nb (at. %) annealed for 1 h at 1300°C.

^cNi-49.05Al-1.5Mo-0.4Ta (at. %) annealed for 1 h at 1200°C.

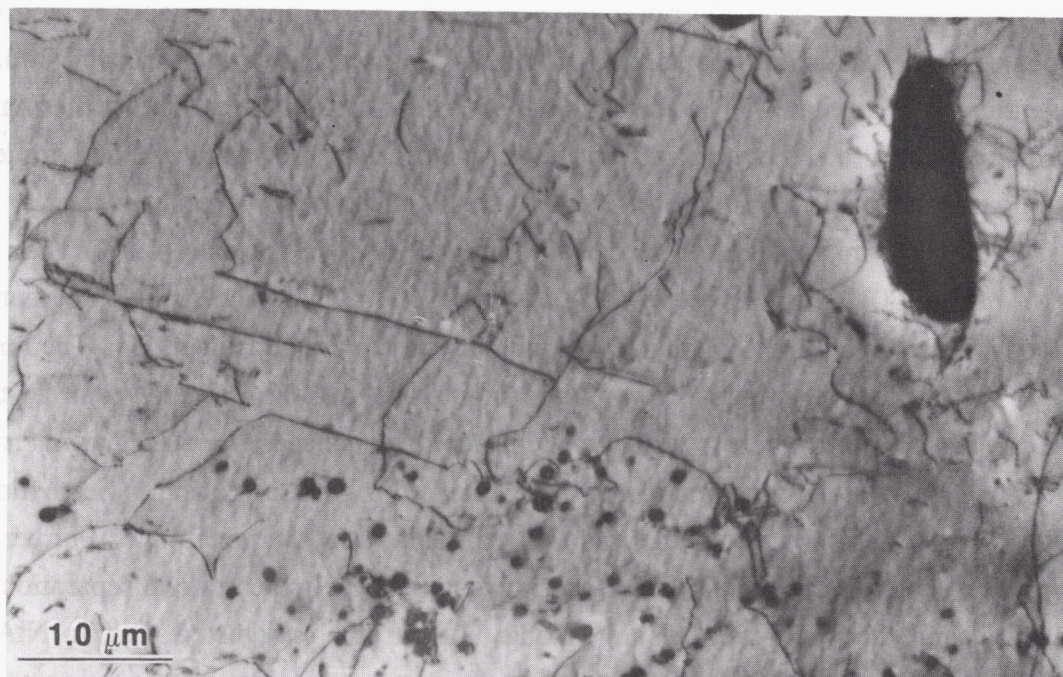


Fig. 9. TEM micrograph of alloy NAL-55 after an anneal of 1 h at 1200°C and a strain of 1.3% showing precipitate and dislocation distribution.

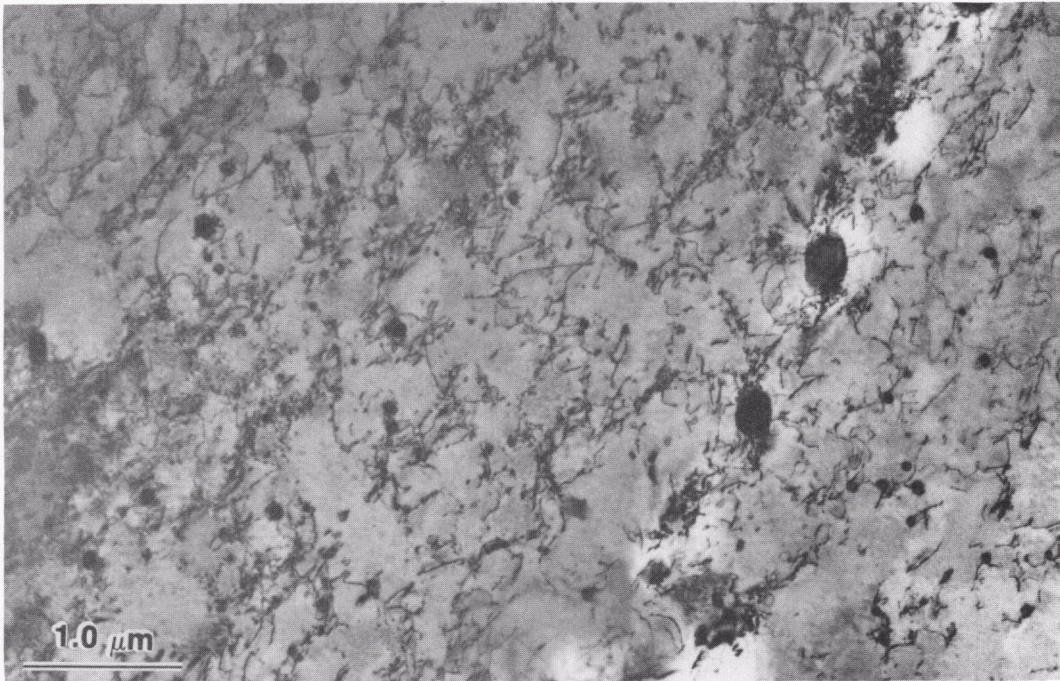
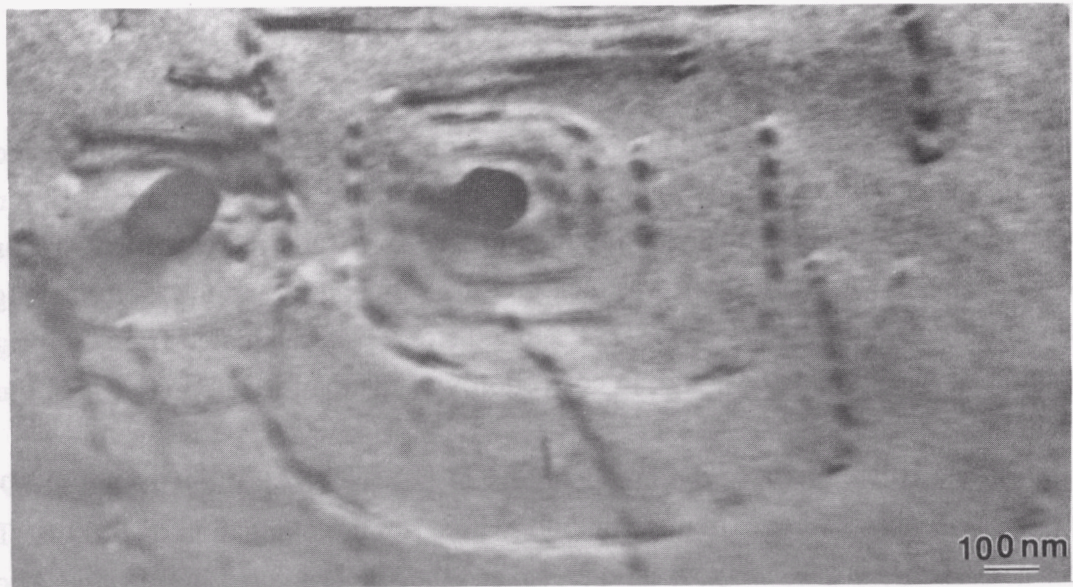


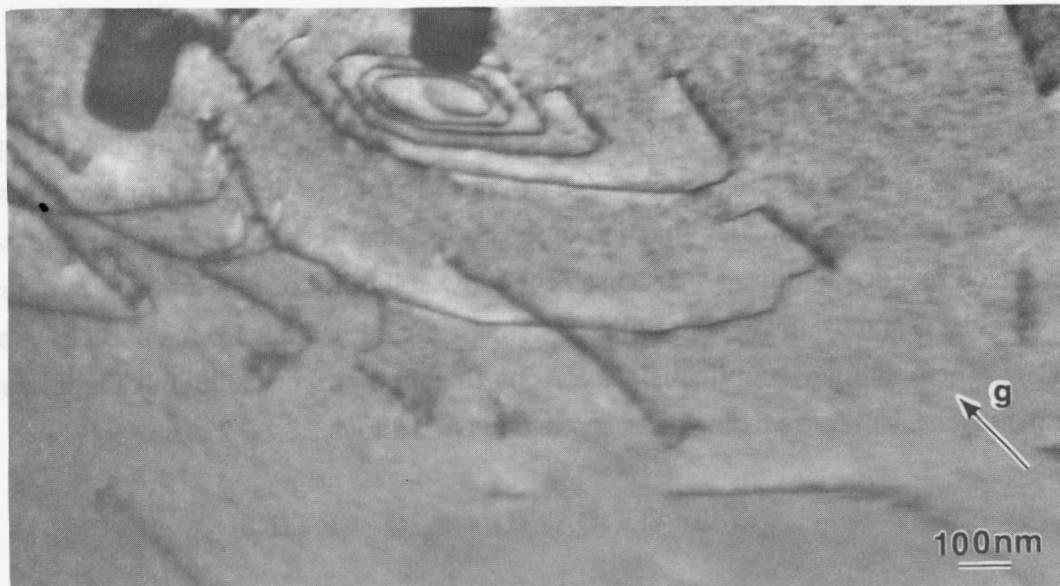
Fig. 10. TEM micrograph of alloy NAL-61 after an anneal of 1 h at 1300°C and a strain of 2.9%.

specimens examined. Dislocations also appear to have been punched out from precipitates (see, for example, the largest precipitate in Fig. 9). Loops are known to form usually on second-phase particles in aluminum-rich NiAl alloys through a vacancy condensation mechanism.³⁴ Voids and loops have also been reported for stoichiometric NiAl,³⁵ again nucleating on precipitates. The formation of loops or voids is dependent on thermal history, especially quench rate. Burgers vectors and slip planes were also analyzed, and limited results indicate that the dislocations in Figs. 9 and 10 are all of the $\langle 100 \rangle$ type.

Figure 11 shows such a dislocation spiral in NAL-59 strained 0.5%. The spiral in Fig. 11 has a $[001]$ Burgers vector and lies on a (001) plane. The straight segments of the dislocation line are along $[100]$ and $[010]$ and thus are a prismatic edge loop. The micrograph in Fig. 11(a) is looking straight down on the habit plane, and the Burgers vector is straight up (and the dislocation therefore shows residual contrast since $g \cdot b = 0$). The micrograph in Fig. 11(b) shows the same spiral, though in a tilted configuration (electron beam along $[101]$ and $g = [\bar{1}01]$), and shows how one end of the spiral starts at the precipitate. Further tilting to a direction such that the spiral is edge-on shows more clearly the vertical separation between the spiral and the precipitate. Yang, Dodd, and Strutt³⁵ suggested that, in NiAl alloys, formation of dislocations, usually by nucleating on precipitates through thermal history, allowed easier deformation to take place through a mechanism of converting the prismatic loops to dislocations involved in the slip process.



(a)



(b)

Fig. 11. TEM micrograph of a dislocation spiral in NAL-59 that nucleated on a second-phase precipitate from a vacancy condensation mechanism. The spiral is a prismatic edge loop with a Burgers vector of $[001]$. Figure 11(a) is looking straight on the (001) habit plane of the spiral. The dislocation is in residual contrast since $g \cdot b = 0$. In Fig. 11(b), the specimen is tilted so that the intersection of the spiral with the precipitate can be seen. The electron beam direction is $[101]$ and $g = [\bar{1}01]$.

8. CREEP PROPERTIES OF NiAl ALLOYS

Creep properties of NiAl alloys were determined at applied stresses of 69 and 138 MPa at 816°C (1500°F) in air. All buttonhead specimens with a dimension of 3.18 mm diam by 17.8 mm long were heat treated to produce a partially or fully recrystallized structure prior to creep testing. The creep strain was measured by a dial gage, and the rupture elongation was determined at room temperature. The applied stress was calculated from the original cross section of alloy specimens, and no correction was made on reduction of area during creep testing.

Table 10 summarizes the creep results of ternary NiAl alloys tested at 69 MPa and 816°C. All alloys were extremely ductile, with a rupture elongation over 60%. The binary NiAl (NAL-31) is extremely weak in creep, and the alloy ruptured in 0.1 min. Alloying with 2% Fe gives a small increase in the rupture life. Among the ternary elements added, vanadium is most effective in extending the rupture life and reducing the creep rate of NiAl. Tungsten ranks second in improving creep resistance.

Creep properties obtained at 138 MPa and 816°C are summarized in Table 11 for Mo-modified NiAl alloys with and without additions of niobium, tantalum, and vanadium. Additions of molybdenum give a moderate increase in the rupture life of NiAl. The addition of niobium and tantalum to 1.5% Mo alloys is most effective in improving the creep properties. As a matter of fact, alloying with 1% Ta extends the rupture life by four orders of magnitude. This result clearly indicates that the creep properties of NiAl alloys can be dramatically improved by alloy additions. Because of the low solubility of niobium and tantalum in NiAl (see Tables 3 and 9), the benefit of these elements mainly comes from a particle-strengthening effect. The pinning of mobile dislocations by fine niobium- or tantalum-rich precipitates may be the mechanism for reducing the creep rate in NiAl alloys.

9. OXIDATION PROPERTIES

Oxidation properties of NiAl alloys containing molybdenum (NAL-58) and molybdenum combined with Nb (NAL-59), Ta (NAL-61), and V (NAL-72) were determined by exposure to air for up to 500 h at 800 and 1000°C, respectively. Disk specimens were first heat-treated for 1 h at 1100°C plus 1 h at 800°C prior to air exposure. The alloy specimens were periodically removed from furnaces and cooled to room temperature for weight measurements.

Table 10. Creep properties of NiAl alloys tested at 68.9 MPa (10 ksi) and 816°C (1500°F) in air

Alloy number	Alloy concentration (at. %)	Rupture life (h)	Minimum creep rate (%/h)	Rupture elongation (%)
NAL-31	0	0.1	257.0	63.0
NAL-64	2 Fe	0.5	57.0	75.3
NAL-44	0.4 Mo	22.0	0.90	77.0
NAL-58	1.5 Mo	41.3	0.57	64.3
NAL-51	0.4 W	57.1	0.43	52.9
NAL-49	0.4 V	202.0	0.042	62.0

Table 11. Creep properties of NiAl alloys tested at 138 MPa (20 ksi) and 816°C (1500°F)

Alloy number	Alloy concentration (at. %)	Rupture life (h)	Minimum creep rate (%/h)	Rupture elongation (%)
NAL-31	0	<0.1	--	--
NAL-55	0.7 Mo	3.7	1.7	33.5
NAL-66	2.0 Mo	4.5	2.4	30.2
NAL-59	1.5 Mo + 0.4 Nb	56.8	--	45.6
NAL-60	1.5 Mo + 1.0 Nb	231.0	0.015	50.4
NAL-61	1.5 Mo + 0.4 Ta	18.4	--	54.0
NAL-62	1.5 Mo + 1.0 Ta	715.0	0.0086	57.1
NAL-72	1.5 Mo + 0.4 V	1.2	10.0	40.3
NAL-73	1.5 Mo + 1.0 V	15.4	0.50	50.8

Figures 12 and 13 show a plot of weight change in the alloys as a function of exposure time at 800 and 1000°C, respectively. All the alloys exhibited very low weight gain and showed no indication of spalling. At 800°C, NAL-61 containing tantalum showed the highest weight gain, while NAL-59 containing niobium showed the lowest weight gain. At 1000°C, the weight gain is almost the same for all the alloys. Note that there is no major difference in oxidation rate at 800 and 1000°C, indicating excellent oxidation resistance of the NiAl alloys.

10. SUMMARY AND CONCLUSIONS

The objective of this program is to study alloying effects in near-stoichiometric NiAl for the purpose of improving its mechanical and metallurgical properties for structural applications at high temperatures. Ternary additions of 12 elements, including Fe, Mo, Cr, Ga, Ti, V, Y, W, Mn, Cu, Ag, and Zn, were added to NiAl, and selection of the alloying elements was based on considerations of electronic structure, atom bonding, solubility limit, and APB energy. The alloy ingots containing up to 10 at. % alloying elements were prepared and fabricated into rod stock by hot extrusion at 900 to 1050°C.

Our tensile tests indicate that, among the alloying elements added to NiAl, molybdenum is found to be most effective in improving both the ductility at room temperature and strength at elevated temperatures. Alloying with $1.0 \pm 0.6\%$ Mo almost doubles the room-temperature tensile ductility of NiAl and triples its yield strength at 1000°C. The solubility of molybdenum is low in NiAl, and second-phase particles were observed in the alloys containing more than 0.1 at. % Mo. The particles are effective in retarding recrystallization, and alloying with 0.4% Mo raises the recrystallization temperature of NiAl from 800 to 1200°C.

The high-temperature strength and creep resistance of Mo-modified NiAl alloys can be substantially improved by alloying with up to 1 at. % Nb or Ta. At 1000°C, niobium is most effective in strengthening NiAl, and a fivefold increase in yield strength is achieved by adding 1% Nb. Because of the low solubility of niobium and tantalum, fine precipitates (0.25 to 1 μm) form in Nb- and Ta-modified alloys containing molybdenum additions, as evidenced by TEM studies. Burgers vectors were analyzed, and limited results indicate that dislocations in the alloys are of the $\langle 100 \rangle$ type. The fine precipitates are expected to contribute to pinning dislocations and enhancing the strength of these alloys. Creep tests at 138 MPa and 816°C showed that alloying with 1% Nb or Ta extends the rupture life of NiAl alloys containing 1.5% Mo by four orders of magnitude. All the alloys exhibited excellent oxidation resistance at 800 and 1000°C.

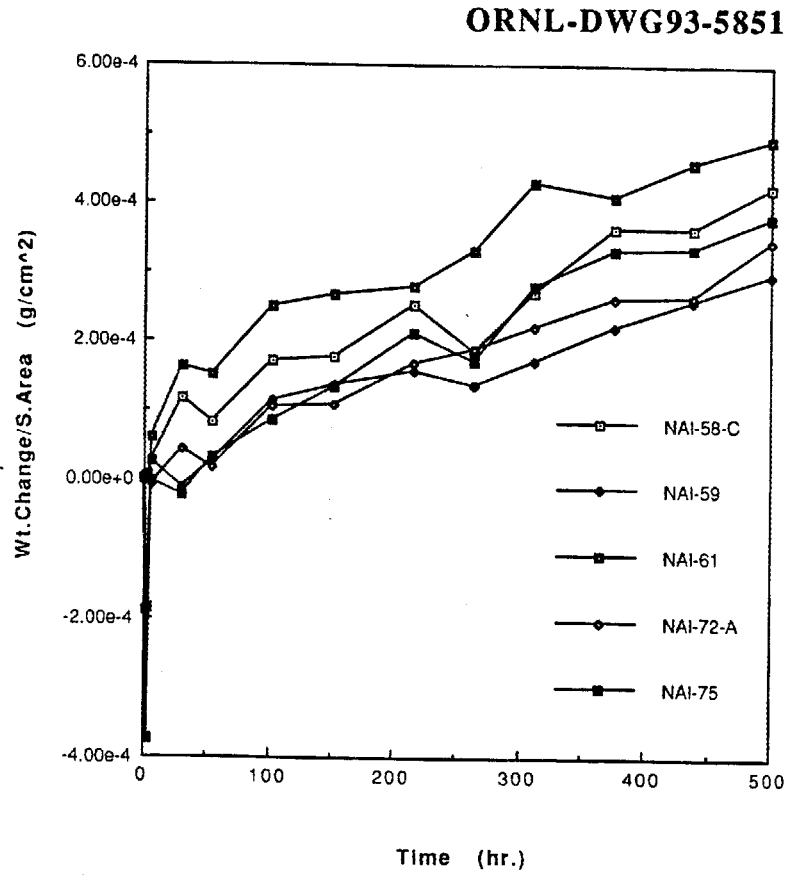


Fig. 12. Plot of weight change as a function of exposure time for NiAl alloys exposed to air at 800°C.

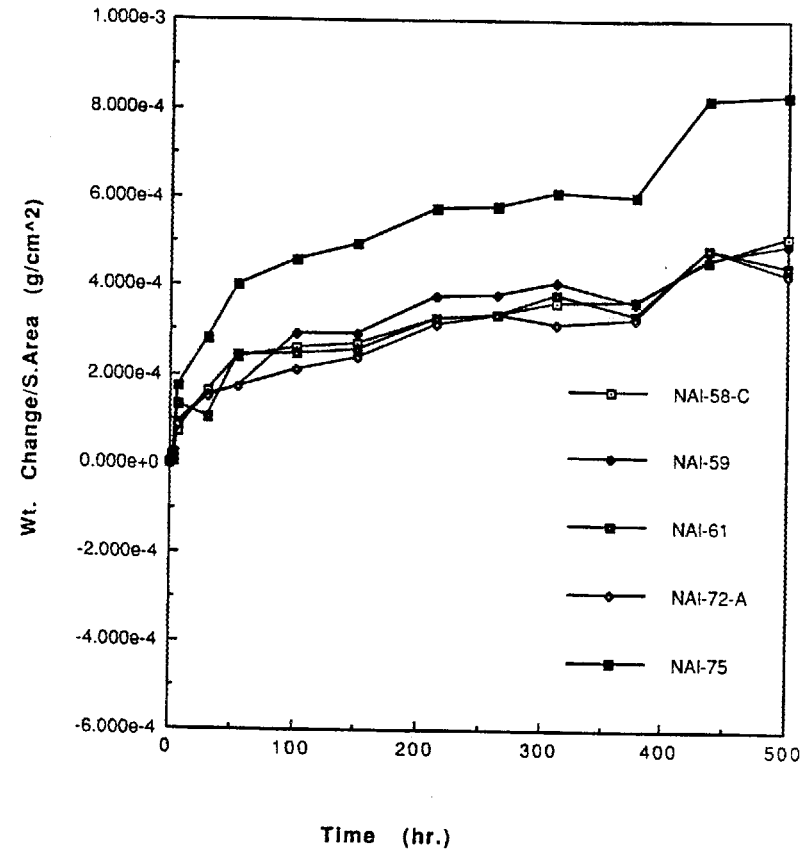


Fig. 13. Plot of weight change as a function of exposure time for NiAl alloys exposed to air at 1000°C.

This study of alloying effects provides a critical input for the alloy design of ductile and strong NiAl alloys. Our study identified the following alloy composition (at. %) with promising properties:



Note that the nickel and aluminum concentrations in the alloy should be kept at the same level.

11. ACKNOWLEDGMENTS

The authors are grateful to M. H. Yoo, C. G. McKamey, and P. Angelini for review and valuable discussions and D. H. Pierce, L. M. Pike, P. A. Ferguson, T. Henson, J. D. Vought, K. S. Blakely, and C. E. Dunn for technical assistance. Thanks are also due to Debbie McCoy, Fay Christie, and Connie Dowker for manuscript preparation; Lisa Kendrick for final report preparation; and Kathy Spence for editing.

12. REFERENCES

1. *Binary Alloy Phase Diagrams*, ed. T. B. Massalski, Vols. 1 and 2, American Society for Metals, Materials Park, Ohio, 1986.
2. E. A. Aitken, pp. 491-516 in *Intermetallic Compounds*, ed. J. H. Westbrook, Wiley, New York, 1967.
3. J. L. Smialek, *Metall. Trans. A* **9A**, 309 (1978).
4. J. Jedlinski and S. Miowic, *Mater. Sci. Eng.* **87**, 281 (1987).
5. C. A. Barrett, *Oxid. Met.* **30**, 361 (1988).
6. *High-Temperature Ordered Intermetallic Alloys*, proceedings of Materials Research Society symposium, Vol. 39, ed. C. C. Koch, C. T. Liu, and N. S. Stoloff, Materials Research Society, Pittsburgh, 1985.
7. *High-Temperature Ordered Intermetallic Alloys II*, proceedings of Materials Research Society symposium, Vol. 81, ed. N. S. Stoloff, C. C. Koch, C. T. Liu, and O. Izumi, Materials Research Society, Pittsburgh, 1987.
8. *High-Temperature Ordered Intermetallic Alloys III*, proceedings of Materials Research Society symposium, Vol. 133, ed. C. T. Liu, A. I. Taub, N. S. Stoloff, and C. C. Koch, Materials Research Society, Pittsburgh, 1989.
9. A. Ball and R. E. Smallman, *Acta Metall.* **14**, 1517 (1966).

10. N. J. Zaluzec and H. L. Fraser, *Scr. Metall.* **8**, 1049 (1974).
11. I. Baker and E. M. Schulson, *Metall. Trans. A* **15A**, 1129 (1984).
12. E. M. Grala, pp. 358-404 in *Mechanical Properties of Intermetallic Compounds*, ed. J. H. Westbrook, Wiley, New York, 1960.
13. K. H. Hahn and K. Vedula, *Scr. Metall.* **23**, 7 (1989).
14. A. G. Rozner and R. J. Wasilewski, *J. Inst. Met.* **94**, 169 (1966).
15. E. P. George and C. T. Liu, *J. Mater. Res.* **5**, 754 (1990).
16. E. P. George, C. T. Liu, and J. J. Liao, in *Alloy Phase Stability and Design*, proceedings of Materials Research Society symposium, Vol. 186, eds. G. M. Stocks, D. P. Pope, and A. F. Giamei, Materials Research Society, Pittsburgh, 1990.
17. K. Vedula and J. R. Stephens, p. 381 in *High Temperature Ordered Intermetallic Alloys*, Vol. 81, eds. N. S. Stoloff, C. C. Koch, C. T. Liu, and O. Izumi, Materials Research Society, Pittsburgh, 1987.
18. A. J. Bradley and A. Taylor, *Proc. R. Soc. London, A* **136**, 210 (1932).
19. A. J. Bradley and A. Taylor, *Proc. R. Soc. London, A* **159**, 56 (1937).
20. N. Ridley, *J. Inst. Met.* **94**, 255 (1966).
21. M. J. Cooper, *Philos. Mag.* **8**, 805 (1963).
22. J. H. Westbrook, *J. Electrochem. Soc.* **103**, 54 (1956).
23. C. T. Liu, C. L. White, and J. A. Horton, *Acta Metall.* **33**, 213-19 (1985).
24. T. Takasugi, E. P. George, D. P. Pope, and O. Izumi, *Scr. Metall.* **19**, 551-56 (1985).
25. T. Ogura, S. Hanada, T. Masumoto, and O. Izumi, *Metall. Trans. A* **16A**, 441-43 (1985).
26. K. Aoki and O. Izumi, *Nippon Kinzoku Gakkaishi* **43**, 1190 (1979).
27. A. I. Taub, S. C. Huang, and K. M. Chang, *Metall. Trans. A* **15A**, 399 (1984).
28. D. G. Pettifor, *New Sci.* **110**(1510), 48-53 (1986).
29. D. G. Pettifor, *J. Phys. C* **19**, 285-313 (1986).
30. D. G. Pettifor and R. Podloucky, *Phys. Rev. Lett.* **55**, 261 (1985).
31. D. B. Miracle, S. Russell, and C. C. Law, pp. 225-30 in *High-Temperature Ordered Intermetallic Alloys III*, proceedings of Materials Research Society symposium, Vol. 133, ed. C. T. Liu, A. I. Taub, N. S. Stoloff, and C. C. Koch, Materials Research Society, Pittsburgh, 1989.

32. R. Darolia, D. F. Lahrman, R. D. Field, and A. J. Freeman, pp. 113-18 in *High-Temperature Ordered Intermetallic Alloys III*, proceedings of Materials Research Society symposium, Vol. 133, ed. C. T. Liu, A. I. Taub, N. S. Stoloff, and C. C. Koch, Materials Research Society, Pittsburgh, 1989.

33. K. Vedula, V. Pathare, I. Aslamidis, and R. H. Titran, pp. 411-21 in *High-Temperature Ordered Intermetallic Alloys*, proceedings of Materials Research Society symposium held at Boston, Maine, Vol. 39, ed. C. C. Koch, C. T. Liu, and N. S. Stoloff, Materials Research Society, Pittsburgh, 1985.

34. G. W. Marshall and J. O. Brittain, *Metall. Trans. A* **6A**, 921-26 (1975).

35. W. Yang, R. A. Dodd, and P. R. Strutt, *Metall. Trans. A* **3**, 2049-2054 (1972).

INTERNAL DISTRIBUTION

- | | | | |
|--------|-------------------------------|--------|------------------------------|
| 1-2. | Central Research Library | 46. | H. Lin |
| 3. | Document Reference Library | 47-51. | C. T. Liu |
| 4-5. | Laboratory Records Department | 52. | K. C. Liu |
| 6. | Laboratory Records, ORNL-RC | 53. | G. M. Ludtka |
| 7. | ORNL Patent Section | 54. | G. M. Ludtka |
| 8-10. | M&C Records Office | 55. | P. J. Maziasz |
| 11. | D. J. Alexander | 56. | H. E. McCoy, Jr. |
| 12. | J. D. Allen, Jr. | 57. | C. G. McKamey |
| 13. | P. F. Becher | 58. | M. K. Miller |
| 14. | E. E. Bloom | 59. | R. N. Morris |
| 15. | R. A. Bradley | 60. | M. Olszewski |
| 16. | C. R. Brinkman | 61. | W. D. Porter |
| 17. | W. H. Butler | 62. | P. L. Rittenhouse |
| 18. | R. S. Carlsmith | 63. | M. L. Santella |
| 19. | D. F. Craig | 64. | J. H. Schneibel |
| 20. | S. A. David | 65. | P. S. Sklad |
| 21. | R. M. Davis | 66. | V. K. Sikka |
| 22. | J. H. DeVan | 67. | C. J. Sparks, Jr. |
| 23. | H. W. Hayden | 68. | V. J. Tennery |
| 24-28. | E. P. George | 69. | P. F. Tortorelli |
| 29. | R. L. Heestand | 70. | S. Viswanathan |
| 30-34. | J. A. Horton | 71. | J. R. Weir, Jr. |
| 35. | L. L. Horton | 72. | Y. A. Chang (Consultant) |
| 36. | C. R. Hubbard | 73. | H. W. Foglesong (Consultant) |
| 37. | T. J. Huxford | 74. | J. J. Hren (Consultant) |
| 38. | J. R. Keiser | 75. | M. L. Savitz (Consultant) |
| 39. | E. A. Kenik | 76. | J. G. Simon (Consultant) |
| 40. | J. F. King | 77. | K. E. Spear (Consultant) |
| 41-45. | E. H. Lee | | |

EXTERNAL DISTRIBUTION

78. CARPENTER TECHNOLOGY CORPORATION, 101 West Bern St.,
P.O. Box 4662, Reading, PA 19612-4662
- N. Fiore
79. COORS CERAMIC COMPANY, Technical Operations and Engineering,
600 Ninth St., Golden, CO 80401
- D. Wirth, Vice President

80. DARMOUTH COLLEGE, Thayer School of Engineering, Hanover, NH 03755
I. Baker
81. DOW CHEMICAL COMPANY, INC., Central Research, Catalysis Laboratory,
1776 Building, Midland, MI 49674
R. D. Varjian
82. ELECTRICAL POWER RESEARCH INSTITUTE, Nuclear Plant Corrosion
Control, 3412 Hillview Ave., Palo Alto, CA 94303
M. M. Behravesh
83. LEHIGH UNIVERSITY, Bethlehem, PA 18015
A. K. MacPherson
- 84-85. LOS ALAMOS NATIONAL LABORATORY, P. O. Box 1663, G7771,
Los Alamos, NM 87545
J. J. Petrovic
A. D. Rollett
86. NATIONAL INSTITUTE OF STANDARDS AND TECHNOLOGY,
Metallurgy Division, Building 223, Room B248, Gaithersburg, MD 20899
R. E. Ricker
87. NAVAL RESEARCH LABORATORY, Materials Science and Component
Technology, Code 6000, Building 43, Room 212, Washington,
DC 20375-5000
B. B. Rath, Associate Director of Research
88. NORTH CAROLINA STATE UNIVERSITY, Department of Materials
Engineering, Yarborough Dr., Raleigh, NC 27695-7907
C. C. Koch
89. UNIVERSITY OF CINCINNATI, Materials Science and Engineering
Department, ML 012, Cincinnati, OH 45221
J. A. Sekhar
90. UNIVERSITY OF TENNESSEE, Department of Materials Science and
Engineering, Knoxville, TN 37996-2200
B. F. Oliver

91. VANDER LINDEN AND ASSOCIATES, 5 Brassie Way, Littleton, CO 80123
C. R. Vander Linden
92. WISCONSIN CENTRIFUGAL, 905 E. St. Paul Ave., Waukesha,
WI 53188-3898
T. J. Devine
- 93-94. U.S. DOE, Forrestal Building, 1000 Independence Ave., SW, Washington,
DC 20585
M. E. Gunn, Jr. (CE-232)
P. H. Salmon-Cox (CE-23)
95. U.S. DOE, ADVANCED INDUSTRIAL CONCEPTS DIVISION, Advanced
Industrial Concepts Materials Program, 1000 Independence Ave., SW,
Washington, DC 20585
C. A. Sorrell (CE-232)
- 96-97. U.S. DOE, OAK RIDGE FIELD OFFICE, P.O. Box 2008, Oak Ridge,
TN 37831
Deputy Assistant Manager for Energy Research and Development
E. E. Hoffman
- 98-99. U.S. DOE, OFFICE OF SCIENTIFIC AND TECHNICAL INFORMATION,
P.O. Box 62, Oak Ridge, TN 37831
For distribution by microfiche as shown in DOE/OSTI-4500,
Distribution Category UC-310 [Industrial Programs (General)]

